



**Analyses of
uncertainties and
scaling of
groundwater level
fluctuations**

X. Liang and Y.-K. Zhang

Analyses of uncertainties and scaling of groundwater level fluctuations

X. Y. Liang^{1,2} and Y.-K. Zhang^{1,2,3}

¹Center for Hydrosiences Research, Nanjing University, Nanjing, Jiangsu 210093, China

²School of Earth Sciences and Engineering, Nanjing University, Nanjing, Jiangsu 210093, China

³Department of Geoscience, University of Iowa, Iowa City, Iowa 52242, USA

Received: 26 November 2014 – Accepted: 9 December 2014 – Published: 6 January 2015

Correspondence to: Y.-K. Zhang (y kzhang@nju.edu.cn)

Published by Copernicus Publications on behalf of the European Geosciences Union.

Title Page

Abstract

Introduction

Conclusions

References

Tables

Figures



Back

Close

Full Screen / Esc

Printer-friendly Version

Interactive Discussion



Abstract

Analytical solutions for the variance, covariance, and spectrum of groundwater level, $h(x, t)$, in an unconfined aquifer described by a linearized Boussinesq equation with random source/sink and initial and boundary conditions were derived. It was found that in a typical aquifer the error in $h(x, t)$ in early time is mainly caused by the random initial condition and the error reduces as time progresses to reach a constant error in later time. The duration during which the effect of the random initial condition is significant may last a few hundred days in most aquifers. The constant error in $h(x, t)$ in later time is due to the combined effects of the uncertainties in the source/sink and flux boundary: the closer to the flux boundary, the larger the error. The error caused by the uncertain head boundary is limited in a narrow zone near the boundary and remains more or less constant over time. The aquifer system behaves as a low-pass filter which filters out high-frequency noises and keeps low-frequency variations. Temporal scaling of groundwater level fluctuations exists in most part of a low permeable aquifer whose horizontal length is much larger than its thickness caused by the temporal fluctuations of areal source/sink.

1 Introduction

Groundwater level or hydraulic head (h) is the main driving force for water flow and advective contaminant transport in aquifers and thus the most important variable studied in groundwater hydrology and its applications. Knowledge about h is critical in dealing with groundwater-related environmental problems, such as over-pumping, subsidence, sea water intrusion, and contamination. One often found that the data about groundwater level is limited or unavailable in a hydrogeological investigation. In such cases the groundwater level distribution and its temporal variation are usually obtained with an analytical or numerical solution to a groundwater flow model.

HESSD

12, 1–23, 2015

Analyses of uncertainties and scaling of groundwater level fluctuations

X. Liang and Y.-K. Zhang

Title Page

Abstract

Introduction

Conclusions

References

Tables

Figures

⏪

⏩

◀

▶

Back

Close

Full Screen / Esc

Printer-friendly Version

Interactive Discussion

Analyses of uncertainties and scaling of groundwater level fluctuations

X. Liang and Y.-K. Zhang

Title Page

Abstract

Introduction

Conclusions

References

Tables

Figures

◀

▶

◀

▶

Back

Close

Full Screen / Esc

Printer-friendly Version

Interactive Discussion



Spatiotemporal variations of groundwater levels calculated or simulated with the analytical or numerical solutions are inherently erroneous. The main sources of errors include the simplification or approximation in a conceptual model and the uncertainties in the model parameters. Problems in conceptualization or model structure were dealt with by many researchers (Neuman, 2003; Rojas et al., 2008, 2010; Ye et al., 2008; Refsgaard et al., 2007; Zeng et al., 2013). The uncertainties in model parameters were investigated (Beven and Binley, 1992; Vrugt et al., 2003; Neuman et al., 2012). The uncertainty in groundwater level has been one of the main research topics in stochastic subsurface hydrology for more than three decades. Most of these studies were focused on the spatial variability of groundwater level due to aquifers' heterogeneity (Dagan, 1989; Gelhar, 1993; Zhang, 2002). Little attention has been given to the uncertainties in groundwater level due to temporal variations of hydrological processes, e.g., recharge, evapotranspiration, discharge to a river, and river stage.

Uncertainties of groundwater level fluctuations have been studied by Zhang and Li (2005, 2006) and most recently by Liang and Zhang (2013). Based on a linear reservoir model with a white noise or temporally-correlated recharge process, Zhang and Li (2005, 2006) derived the variance and covariance of $h(t)$ by considering only a random source or sink process assuming deterministic initial and boundary conditions. Liang and Zhang (2013) extended the studies of Zhang and Li (2005, 2006) and carried out non-stationary spectral analysis and Monte Carlo simulations using a linearized Boussinesq equation, and investigated the temporospatial variations of groundwater level. However, the only random process considered by Liang and Zhang (2013) is the source/sink. Temporal scaling of groundwater levels discovered first by Zhang and Schilling (2004) was verified in several studies (Zhang and Li, 2005, 2006; Bloomfield and Little, 2010; Zhang and Yang, 2010; Zhu et al., 2012; Schilling and Zhang, 2012). However, we do not know the effect of random boundary conditions on temporal scaling of groundwater levels.

In this study we extended above-mentioned work by considering the groundwater flow in a bounded aquifer described by a linearized Boussinesq equation with a ran-

Analyses of uncertainties and scaling of groundwater level fluctuations

X. Liang and Y.-K. Zhang

Title Page

Abstract

Introduction

Conclusions

References

Tables

Figures

◀

▶

◀

▶

Back

Close

Full Screen / Esc

Printer-friendly Version

Interactive Discussion

dom source/sink as well as random initial and boundary conditions since the latter processes are known with uncertainties. The objectives of this study are (1) to derive analytical solutions for the covariance, variance and spectrum of groundwater level, and (2) to investigate the individual and combined effects of these random processes on uncertainties and scaling of $h(x, t)$. In the following we will first present the formulation and analytical solutions, then discuss the results, and finally draw some conclusions.

2 Formulation and solutions

Under the Dupuit assumption, the one-dimensional transient groundwater flow in an unconfined aquifer near a river can be approximated with the linearized Boussinesq equation (Bear, 1972) with the initial and boundary conditions, i.e.,

$$T \frac{\partial^2 h}{\partial x^2} + W(t) = S_Y \frac{\partial h}{\partial t} \quad (1a)$$

$$h(x, t)|_{t=0} = H_0(x); \quad T \frac{\partial h}{\partial x} \Big|_{x=0} = Q(t); \quad h(x, t)|_{x=L} = H(t) \quad (1b)$$

where T [$L T^{-1}$] is the transmissivity, h [L] is the hydraulic head or groundwater level above the bottom of the aquifer which is assumed to be horizontal, $W(t)$ [$L T^{-1}$] is the time-dependent source/sink term representing areal recharge or evapotranspiration, S_Y is the specific yield, $H_0(x)$ [L] is the initial condition, $Q(t)$ [$L^2 T^{-1}$] is the time-dependent flux at the left boundary, $H(t)$ [L] is the time-dependent water level at the right boundary, L [L] is distance from the left to the right boundary, x [L] is the coordinate, and t [T] is time. In this study the initial head $H_0(x)$ is taken to be a spatially random variable, and the source/sink, $W(t)$, the flux to the left boundary, $Q(t)$, and the head at the right boundary, $H(t)$, are all taken to be temporally random processes and spatially deterministic. The parameters T and S_Y are taken to be constant.

The groundwater level, $h(x, t)$, the three random processes, $W(t)$, $Q(t)$, and $H(t)$, and the random variable, $H_0(x)$, are expressed in terms of their respective ensemble

means plus small perturbations,

$$h(x, t) = \langle h(x, t) \rangle + h'(x, t) \quad (2a)$$

$$W(t) = \langle W(t) \rangle + W'(t); \quad Q(t) = \langle Q(t) \rangle + Q'(t) \quad (2b)$$

$$H(t) = \langle H(t) \rangle + H'(t); \quad H_0(x) = \langle H_0(x) \rangle + H'_0(x) \quad (2c)$$

5 where $\langle \rangle$ stands for ensemble average and $'$ for perturbation. Although the initial condition $H_0(x)$ in Eq. (1) can be any function, it is appropriate to set it to be the steady-state solution to the one-dimensional transient groundwater flow equation, i.e., $H_0(x) = h_0 + 0.5W_0(L^2 - x^2)/T$, where h_0 [L] is the constant groundwater level at the right boundary and W_0 [$L T^{-1}$] is the spatially constant recharge rate (Liang and Zhang, 2012). Since h_0 is taken to be constant, the source of the uncertainty in the initial head $H_0(x)$ is due to random W_0 only. Thus, the mean and perturbation of $H_0(x)$ can be written as, $\langle H_0(x) \rangle = h'_0(x) = 0.5W'_0(L^2 - x^2)/T$, respectively. By substituting Eq. (2), $\langle H_0(x) \rangle$, and $H'_0(x)$ into Eq. (1) and taking expectation, one obtains the mean flow equation with the mean initial and boundary conditions as

$$15 \quad T \frac{\partial^2 \langle h \rangle}{\partial x^2} + \langle W \rangle = S_Y \frac{\partial \langle h \rangle}{\partial t} \quad (3a)$$

$$\langle h(x, 0) \rangle = h_0 + \frac{\langle W_0 \rangle}{2T} (L^2 - x^2); \quad T \frac{\partial \langle h \rangle}{\partial x} \Big|_{x=0} = \langle Q \rangle; \quad \langle h(L, t) \rangle = \langle H(t) \rangle \quad (3b)$$

Subtracting Eq. (3) from Eq. (1) leads to the following perturbation equation with the initial and boundary conditions

$$T \frac{\partial^2 h'}{\partial x^2} + W' = S_Y \frac{\partial h'}{\partial t} \quad (4a)$$

$$20 \quad h'(x, 0) = \frac{W'_0}{2T} (L^2 - x^2); \quad T \frac{\partial h'}{\partial x} \Big|_{x=0} = Q'; \quad h'(L, t) = H'(t) \quad (4b)$$

HESSD

12, 1–23, 2015

Analyses of uncertainties and scaling of groundwater level fluctuations

X. Liang and Y.-K. Zhang

Title Page

Abstract

Introduction

Conclusions

References

Tables

Figures

◀

▶

◀

▶

Back

Close

Full Screen / Esc

Printer-friendly Version

Interactive Discussion



The analytical solution to Eq. (4) can be derived with integral-transform methods (Ozisk, 1968) given by

$$h' = \frac{2}{L} \sum_{n=0}^{\infty} e^{-\beta b_n^2 t} \cos(b_n x)$$

$$\left[\frac{(-1)^n}{b_n^3 T} W'_0 + \beta \int_0^t e^{\beta b_n^2 \xi} \left[\frac{(-1)^n}{T b_n} W'(\xi) - \frac{Q'(\xi)}{T} + H'(\xi) (-1)^n b_n \right] d\xi \right] \quad (5)$$

5 where $\beta = T/S_Y$, $b_n = (2n + 1)\pi/(2L)$. Using Eq. (5), the temporal covariance of the groundwater level fluctuations can be derived as

$$C_{hh}(x, t_1; x, t_2) = E[h'(x, t_1)h'(x, t_2)]$$

$$= \frac{4}{L^2} \sum_{m=0}^{\infty} \sum_{n=0}^{\infty} e^{-\beta(b_m^2 t_1 + b_n^2 t_2)} \cos(b_m x) \cos(b_n x) \left[\frac{(-1)^{m+n}}{T^2 b_m^3 b_n^3} \sigma_{W_0}^2 \right. \quad (6)$$

$$\left. + \beta^2 \int_0^{t_1} \int_0^{t_2} e^{\beta(b_m^2 \xi + b_n^2 \rho)} \left[\frac{(-1)^{n+m}}{T^2 b_m b_n} C_{WW}(\xi, \rho) + \frac{C_{QQ}(\xi, \rho)}{T^2} + C_{HH}(\xi, \rho) (-1)^{m+n} b_m b_n \right] d\xi d\rho \right]$$

10 in which $\sigma_{W_0}^2$ is the variance of W_0 , and $C_{WW}(\xi, \rho)$, $C_{QQ}(\xi, \rho)$ and $C_{HH}(\xi, \rho)$ are the temporal auto-covariance of $W(t)$, of $Q(t)$, and $H(t)$, respectively. We assume that $W(t)$, $Q(t)$, and $H(t)$ are uncorrelated in order to simplify our analyses. It is shown in Eq. (6) that the head covariance depends on the variance of W_0 and the covariances of $W(t)$, $Q(t)$, and $H(t)$ and this equation can be evaluated for any random $W(t)$, $Q(t)$, and $H(t)$.

15 We assume that these processes are white noises as employed in previous studies (Gelhar, 1993; Hantush and Marino, 1994; Liang and Zhang, 2013). More realistic randomness of these processes will be considered in future studies.

Analyses of uncertainties and scaling of groundwater level fluctuations

X. Liang and Y.-K. Zhang

Title Page

Abstract

Introduction

Conclusions

References

Tables

Figures

◀

▶

◀

▶

Back

Close

Full Screen / Esc

Printer-friendly Version

Interactive Discussion

Analyses of uncertainties and scaling of groundwater level fluctuations

X. Liang and Y.-K. Zhang

Title Page

Abstract

Introduction

Conclusions

References

Tables

Figures

◀

▶

◀

▶

Back

Close

Full Screen / Esc

Printer-friendly Version

Interactive Discussion



Following Gelhar (1993, p. 34), we express the spectra of $W(t)$, $Q(t)$, and $H(t)$ as $S_{WW} = \sigma_W^2 \lambda_W / \pi$, $S_{QQ} = \sigma_Q^2 \lambda_Q / \pi$, and $S_{HH} = \sigma_H^2 \lambda_H / \pi$, respectively, where σ_W^2 , σ_Q^2 , and σ_H^2 are the variances and λ_W , λ_Q , and λ_H are the correlation time intervals of these three processes, respectively. The corresponding covariance of $W(t)$, $Q(t)$ and $H(t)$ are $C_{WW}(\xi, \rho) = 2\sigma_W^2 \lambda_W \delta(\xi - \rho)$, $C_{QQ}(\xi, \rho) = 2\sigma_Q^2 \lambda_Q \delta(\xi - \rho)$, and $C_{HH}(\xi, \rho) = 2\sigma_H^2 \lambda_H \delta(\xi - \rho)$. Substituting these covariance into Eq. (6) and taking integration, one obtain analytical solution of head covariance

$$C_{hh}(x', t', \tau') = \frac{4\beta L^2}{T^2} \sum_{m=0}^{\infty} \sum_{n=0}^{\infty} \cos(b'_m x') \cos(b'_n x') \left\{ e^{-\left[(b'^2_m + b'^2_n) t' + (b'^2_n - b'^2_m) \frac{\tau'}{2} \right]} \frac{L^2 (-1)^{m+n} \sigma_{W0}^2}{\beta b'^3_m b'^3_n} + 2 \frac{\left(e^{-b'^2_m \tau'} - e^{-2b'^2_m t'} \right)}{(b'^2_m + b'^2_n)} \left[\frac{(-1)^{m+n} \sigma_W^2 \lambda_W}{b'_m b'_n} + \frac{\sigma_Q^2 \lambda_Q}{L^2} + \frac{(-1)^{m+n} b'_m b'_n T^2 \sigma_H^2 \lambda_H}{L^4} \right] \right\} \quad (7)$$

where $\tau' = t'_2 - t'_1$ and $t' = (t'_2 + t'_1)/2$. The analytical solution for the head variance can be obtain by setting $\tau' = 0$

$$\sigma_h^2(x', t') = \frac{4\beta L^2}{T^2} \sum_{m=0}^{\infty} \sum_{n=0}^{\infty} \cos(b'_m x') \cos(b'_n x') \left\{ e^{-\left(b'^2_m + b'^2_n \right) t'} \frac{L^2 (-1)^{m+n} \sigma_{W0}^2}{\beta b'^3_m b'^3_n} + \right. \quad (8)$$

$$\left. 2 \frac{1 - e^{-2b'^2_m t'}}{(b'^2_m + b'^2_n)} \left[\frac{(-1)^{m+n} \sigma_W^2 \lambda_W}{b'_m b'_n} + \frac{\sigma_Q^2 \lambda_Q}{L^2} + \frac{(-1)^{m+n} b'_m b'_n T^2 \sigma_H^2 \lambda_H}{L^4} \right] \right\} \quad (9)$$

where

$$t' = \frac{t}{t_c}; \quad x' = \frac{x}{L}; \quad t_c = \frac{L^2}{\beta}; \quad b'_n = \frac{(2n+1)\pi}{2}$$

in which $t_c (= S_Y L^2 / (KM)) [1 T^{-1}]$ is a characteristic timescale (Gelhar, 1993) where the transmissivity (T) is replaced by the product of the hydraulic conductivity (K) and the average saturated thickness (M) of the aquifer. The characteristic timescale (t_c) is an important parameter and its value for most shallow aquifers is usually larger than 100 day since the horizontal extent of a shallow aquifer is usually much larger than its thickness. For instance, the value of t_c is 250 days for a sandy aquifer with $L = 100$ m, $M = 10$ m, $K = 1$ mday⁻¹, and $S_Y = 0.25$.

The spectral density of $h(x, t)$ can not be derived by ordinary Fourier transform since the head covariance and variance depend on time t' and thus $h(x, t)$ are temporally non-stationary as shown in Eqs. (7) and (8). Priestley (1981) defined the spectral density of non-stationary processes (Wigner spectrum) as the Fourier transform of time-dependent auto-covariance with fixed reference time t and derived time-dependent spectral density. In order to obtain the spectrum of $h(x, t)$, we applied Priestley's method and obtained the time-dependent spectral density (Priestley, 1981; Zhang and Li, 2005; Liang and Zhang, 2013), i.e.,

$$\begin{aligned}
 S_{hh}(x, t, \omega) &= \frac{1}{2\pi} \int_{-\infty}^{\infty} C_{hh}(x, t, \tau) e^{-i\omega\tau} d\tau \\
 &= \sum_{m=0}^{\infty} \sum_{n=0}^{\infty} \cos(b_m x) \cos(b_n x) \frac{2t_c (b_n^2 - b_m^2) e^{-\beta(b_m^2 + b_n^2)t} (-1)^{m+n} \sigma_{W_0}^2}{\beta^2 (b_n^2 - b_m^2)^2 / 4 + \omega^2} \frac{1}{\pi T^2 b_m^3 b_n^3} + \\
 &\quad \sum_{m=0}^{\infty} \sum_{n=0}^{\infty} \cos(b_m x) \cos(b_n x) \frac{8\beta b_m^2}{t_c (b_m^2 + b_n^2)} \frac{1}{\beta^2 b_m^4 + \omega^2} \\
 &\quad \left[\frac{(-1)^{m+n} S_{WW}}{T^2 b_m b_n} + \frac{S_{QQ}}{T^2} + (-1)^{m+n} b_m b_n S_{HH} \right]
 \end{aligned} \tag{10}$$

where ω is angular frequency and $\omega = 2\pi f$, f is frequency, and $i = \sqrt{-1}$. It is seen in Eq. (10) that the spectrum S_{hh} dependent on not only frequency and locations but

HESSD

12, 1–23, 2015

Analyses of uncertainties and scaling of groundwater level fluctuations

X. Liang and Y.-K. Zhang

Title Page

Abstract

Introduction

Conclusions

References

Tables

Figures

◀

▶

◀

▶

Back

Close

Full Screen / Esc

Printer-friendly Version

Interactive Discussion



also time t . The time-dependent term (i.e., first term) in Eq. (10) is caused by the random initial condition and is proportional to $e^{-\beta(b_m^2+b_n^2)t}$ which decay quickly with t . We evaluated the first term in the Eq. (10) by setting $t = 0$ and found that it is much smaller than the second term in Eq. (10). We thus ignored the first term and evaluated the spectrum using the approximation,

$$S_{hh}(x', \omega) = \sum_{m=0}^{\infty} \sum_{n=0}^{\infty} \frac{8\beta b_m'^2 \cos(b_m'x') \cos(b_n'x')}{t_c (b_m'^2 + b_n'^2) (\beta^2 b_m'^4 / L^4 + \omega^2)} \left[\frac{(-1)^{m+n} S_{WW} L^2}{T^2 b_m' b_n'} + \frac{S_{QQ}}{T^2} + \frac{(-1)^{m+n} b_m' b_n' S_{HH}}{L^2} \right] \quad (11)$$

3 Results and discussion

3.1 Variance of groundwater levels

The general expression of the head variance in Eq. (9) depends on the variances of the four random processes, $\sigma_{W_0}^2$, σ_W^2 , σ_Q^2 , and σ_H^2 . In the following we will study their individual and combined effects on the head variation and focus our attention only on the variance of $h(x, t)$. First, we evaluate the effect of the random initial condition due to the random term, W_0 , by setting the variances of $W(t)$, $Q(t)$ and $H(t)$ to be zero, i.e., $\sigma_W^2 = \sigma_Q^2 = \sigma_H^2 = 0$. In this case the dimensionless variance in Eq. (8) reduces to

$$\sigma_h'^2(x', t') = \sum_{m=0}^{\infty} \sum_{n=0}^{\infty} \frac{(-1)^{m+n}}{b_m'^3 b_n'^3} \cos(b_m'x') \cos(b_n'x') e^{-(b_m'^2+b_n'^2)t'} \quad (12)$$

where $\sigma_h'^2 = \sigma_h^2 T^2 / (4L^4 \sigma_{W_0}^2)$. The dimensionless standard deviation of $h(x, t)$, σ_h , or the square root of the dimensionless variance ($\sigma_h'^2$) in Eq. (12) as a function of the

Title Page

Abstract

Introduction

Conclusions

References

Tables

Figures

◀

▶

◀

▶

Back

Close

Full Screen / Esc

Printer-friendly Version

Interactive Discussion

dimensionless time (t') was evaluated and presented in Fig. 1a at five dimensionless locations, $x' = 0, 0.2, 0.4, 0.6,$ and 0.8 . It is shown in Fig. 1a that for a fixed location the standard deviation σ'_h is at its maximum at $t' = 0$ and decreases with time gradually to a negligible number at $t' = 1.0$. This means that the error in $h(x, t)$ predicted by an analytical or numerical solution due to the uncertain initial condition is significant at early time, especially near a flux boundary. The time duration during which the effect of the uncertain initial condition is significant depends on the value of the characteristic timescale (t_c) since $t' = t/t_c$. In most aquifers this duration may last many days. As discussed before, the value of t_c is 250 days for the typical aquifer with $L = 100$ m, $M = 10$ m, $K = 1$ mday⁻¹, and $S_Y = 0.25$. In such an aquifer the effect of the uncertainty in initial condition on $h(x, t)$ is significant during first 250 days ($t' = 1.0$). This duration should be relatively short, however, in a more permeable aquifer whose horizontal extent (L) is relatively smaller than its thickness (M).

The dimensionless standard deviation (σ'_h) based on Eq. (12) as a function of the dimensionless location (x') was presented in Fig. 1b for five dimensionless times, $t' = 0.0, 0.2, 0.4, 0.6,$ and 0.8 . It is seen in Fig. 1b that for a fixed time σ'_h is the largest at the left flux boundary ($x' = 0.0$) and, as expected, becomes zero at the right constant head boundary ($x' = 1.0$) since the right boundary is known. Unlike the rapid decline of σ'_h with t' (Fig. 1a), the change of σ'_h over space (Fig. 1b) is much smoother. As a result, $h(x, t)$ in most part of the aquifer is affected of the uncertain initial condition except near the right constant head boundary. This means that the error in $h(x, t)$ predicted by an analytical or numerical solution due to the uncertain initial condition is significant almost everywhere in the aquifer: the further away from a constant head boundary or the closer to a flux boundary, the larger the error.

HESSD

12, 1–23, 2015

Analyses of uncertainties and scaling of groundwater level fluctuations

X. Liang and Y.-K. Zhang

Title Page

Abstract

Introduction

Conclusions

References

Tables

Figures

◀

▶

◀

▶

Back

Close

Full Screen / Esc

Printer-friendly Version

Interactive Discussion



Secondly, we consider the uncertainty in the areal source/sink term (W) by setting $\sigma_{W_0}^2 = \sigma_Q^2 = \sigma_H^2 = 0$. In this case the dimensionless variance in Eq. (8) reduces to

$$\sigma_h'^2(x', t') = 2 \sum_{m=0}^{\infty} \sum_{n=0}^{\infty} \cos(b'_m x') \cos(b'_n x') \frac{\left(1 - e^{-2b'^2_m t'}\right) (-1)^{m+n}}{(b'^2_m + b'^2_n) b'_m b'_n} \quad (13)$$

where $\sigma_h'^2 = \sigma_h^2 T S_Y / (4L^2 \sigma_W^2 \lambda_W)$. The dimensionless standard deviation (σ_h') based $\sigma_h'^2$ in Eq. (13) as a function of the dimensionless time (t') for the same five locations, $x' = 0.0, 0.2, 0.4, 0.6,$ and 0.8 , was presented in Fig. 1c. Unlike σ_h' due to a random initial condition which decreases with t' (Fig. 1a), σ_h' due to an areal source/sink increase with t' (Fig. 1c) since the initial condition is known in this case. At a fixed location σ_h' is zero initially, gradually increases as time goes, and approaches a constant limit at later time. This means that the error in $h(x, t)$ due to an source/sink is at its minimum at early time and increases with time to become significant and approach a constant limit at later time: the closer to the left flux boundary, the larger the limit. The dimensionless standard deviation (σ_h') vs. the dimensionless location (x') for the dimensionless time, $t' = 0.0, 0.2, 0.4, 0.6,$ and 0.8 , is presented in Fig. 1d. It is seen in Fig. 1d that for a fixed time σ_h' decreases smoothly from the left to the right boundary, indicating that the error in $h(x, t)$ due to the uncertainty in the source/sink is significant almost everywhere in the aquifer but the further away from the constant head boundary or the closer to a flux boundary, the larger the error, similar to the case with the random initial condition (Fig. 1b).

Thirdly, we investigate the effect of the left random flux boundary by setting $\sigma_{W_0}^2 = \sigma_W^2 = \sigma_H^2 = 0$ in Eq. (8). In this case the dimensionless head variance is given by

$$\sigma_h'^2(x', t') = 2 \sum_{m=0}^{\infty} \sum_{n=0}^{\infty} \cos(b'_m x') \cos(b'_n x') \frac{1 - e^{-2b'^2_m t'}}{b'^2_m + b'^2_n} \quad (14)$$

Analyses of uncertainties and scaling of groundwater level fluctuations

X. Liang and Y.-K. Zhang

Title Page

Abstract

Introduction

Conclusions

References

Tables

Figures

⏪

⏩

◀

▶

Back

Close

Full Screen / Esc

Printer-friendly Version

Interactive Discussion



Analyses of uncertainties and scaling of groundwater level fluctuations

X. Liang and Y.-K. Zhang

Title Page

Abstract

Introduction

Conclusions

References

Tables

Figures

◀

▶

◀

▶

Back

Close

Full Screen / Esc

Printer-friendly Version

Interactive Discussion

where $\sigma_h'^2 = \sigma_h^2 T S_Y / (4\sigma_Q^2 \lambda_Q)$. The dimensionless standard deviation (σ_h') based on Eq. (13) as a function of the dimensionless time (t') is plotted in Fig. 1e for $x' = 0.0, 0.2, 0.4, 0.6$ and 0.8 . Similar to the case of the random source/sink in Fig. 1c, at any location σ_h' in Fig. 1e is zero initially because of the deterministic initial condition, increases with time (but at a much faster rate than that in Fig. 1c), and approaches a constant limit earlier than σ_h' in Fig. 1c. This means that the error in $h(x, t)$ due to an uncertain flux boundary is at its minimum at early time and increases quickly with time to approach a constant limit: the closer to the left flux boundary, the larger the limit. The dimensionless deviation (σ_h') as a function of the dimensionless location (x') is plotted in Fig. 1f for $t' = 0.01, 0.1,$ and 1.0 . At any time σ_h' in this case is at its maximum at the left boundary ($x' = 0$), decreases quickly as x' increases, and become zero at the right constant head boundary ($x' = 1$), which is different from the cases with the uncertain initial condition and areal source/sink (Fig. 1b and d). In other words, the error in the head due to the uncertain flux boundary is at its maximum at the boundary but decreases quickly away from the boundary to become insignificant for $x' > 0.8$.

Fourthly, we investigated the effect of the random head boundary by setting $\sigma_{W_0}^2 = \sigma_Q^2 = \sigma_Q^2 = 0$ in Eq. (8). The dimensionless head variance in this case is given by

$$\sigma_h'^2(x', t') = 2 \sum_{m=0}^{\infty} \sum_{n=0}^{\infty} \cos(b'_m x') \cos(b'_n x') \frac{(-1)^{m+n} b'_m b'_n \left(1 - e^{-2b'^2_m t'}\right)}{(b'^2_m + b'^2_n)} \quad (15)$$

where $\sigma_h'^2 = \sigma_h^2 L^2 S_Y / (4T \sigma_H^2 \lambda_H)$. The dimensionless standard deviation (σ_h') based on Eq. (15) as a function of the dimensionless time (t') is provided in Fig. 1g for $x' = 0.0, 0.2, 0.4, 0.6,$ and 0.8 . Similar to the case of the random flux boundary (Fig. 1e), at any location σ_h' is zero at $t' = 0$ and increases with time to quickly approach a constant limit at early time. It is noticed that the top curve in Fig. 1g is for $x' = 0.8$ near the right uncertain head boundary while the top curve in Fig. 1e is for $x' = 0$ at the left uncertain flux boundary. This means that the error in $h(x, t)$ due to the random head

boundary increases with time quickly to approach a constant limit: the closer to the uncertain head boundary, the larger the error. The spatial variation of σ'_h can be clearly observed in Fig. 1h for $t' = 0.01, 0.1, \text{ and } 1.0$. At any time σ'_h is at its maximum at the right boundary ($x' = 1$) where the head is uncertain, decreases quickly away from the boundary. This means that the error in $h(x, t)$ due to the uncertain head boundary is limited in a narrow zone near the boundary ($x' > 0.8$) (Fig. 1h).

Finally, we consider the combined effects of the uncertainties from all four sources, i.e., the initial condition, sources, and flux and head boundaries. The head variance in Eq. (8) is written in the dimensionless form as

$$\sigma'^2_h(x', t') = \sum_{m=0}^{\infty} \sum_{n=0}^{\infty} \cos(b'_m x') \cos(b'_n x') \left\{ e^{-(b'^2_m + b'^2_n)t'} \frac{(-1)^{m+n} \sigma'^2_{W_0}}{b'^3_m b'^3_n} + \frac{2(1 - e^{-2b'^2_m t'})}{(b'^2_m + b'^2_n)} \left[\frac{(-1)^{m+n}}{b'_m b'_n} + \sigma'^2_Q + (-1)^{m+n} b'_m b'_n \sigma'^2_H \right] \right\} \quad (16)$$

where

$$\sigma'^2_h = \frac{\sigma'^2_h T S_Y}{4L^2 \sigma'^2_W \lambda_W}; \quad \sigma'^2_{W_0} = \frac{L^2 S_Y \sigma'^2_{W_0}}{T \sigma'^2_W \lambda_W}; \quad \sigma'^2_Q = \frac{\sigma'^2_Q \lambda_Q}{L^2 \sigma'^2_W \lambda_W}; \quad \sigma'^2_H = \frac{T^2 \sigma'^2_H \lambda_H}{L^4 \sigma'^2_W \lambda_W}$$

The dimensionless variances, $\sigma'^2_{W_0}$, σ'^2_Q and σ'^2_H , need to be specified in order to evaluate the dimensionless $\sigma'^2_h(x', t')$ in Eq. (16). For the typical aquifer mentioned above with $L = 100 \text{ m}$, $T = 10 \text{ m}^2 \text{ day}^{-1}$ (or $K = 1 \text{ m day}^{-1}$ and $M = 10 \text{ m}$) and $S_Y = 0.25$, we set $\sigma'^2_{W_0}/(\sigma'^2_W \lambda_W) = 10^{-1}$, $\sigma'^2_Q \lambda_Q/(\sigma'^2_W \lambda_W) = 10^3$, $\sigma'^2_H \lambda_H/(\sigma'^2_W \lambda_W) = 10^4$ and obtain $\sigma'^2_{W_0} = 25$, $\sigma'^2_Q = 0.1$ and $\sigma'^2_H = 0.01$.

The dimensionless standard deviation (σ'_h) based on Eq. (16) as a function of the dimensionless time (t') is presented in Fig. 2a for $x' = 0.0, 0.2, 0.4, 0.6, \text{ and } 0.8$. It is

observed in Fig. 2a that at any location σ'_h is at its maximum due to the uncertainty in the initial condition, gradually decreases as time goes, and approaches a constant limit at later time ($t' > 0.6$) which is due to the combined effects of the uncertain source/sink and flux and head boundaries. This means that the error in the head in early time is significant if the initial condition is uncertain and reduces as time goes to reach a constant limit or error in later time. The error in head in later time is determined by the uncertainties in the source/sink, flux and head boundaries. The spatial variation of the dimensionless standard deviation (σ'_h) for this case is provided in Fig. 2b for $t' = 0.01, 0.2, 0.4, 0.6,$ and 0.8 . It can be observed that σ'_h is relatively larger near both boundaries. The values of σ'_h at the two boundaries are equivalent (~ 1.3) at early time, say $t' = 0.01$ (the top curve in Fig. 2b) and it reduces slowly away from the flux boundary but quickly away from the head boundary. As time progresses, σ'_h near the head boundary stays more or less the same but reduces significantly in most part of the aquifer. This means that in early time the error in $h(x, t)$ in most part of the aquifer is mainly caused by the initial condition and at later time it is due to the combined effects of the uncertain areal source/sink and flux boundary. The effect of the uncertain head boundary on $h(x, t)$ does not change with time significantly but is limited in a narrow zone near the boundary.

3.2 Spectrum of groundwater levels

We first evaluated S_{hh} in Eq. (11) due to the effect of the white noise flux boundary only by setting $S_{QQ} \neq 0$, $S_{WW} = 0$, and $S_{HH} = 0$. The dimensionless spectrum S_{hh}/S_{QQ} as a function of the frequency (f) was evaluated and presented in the log-log plot (Fig. 3a–c) for three values of t_c (40, 400, and 4000 days) since the value of t_c is 250 days for a sandy aquifer with $L = 100$ m, $M = 10$ m, $K = 1$ m day $^{-1}$, and $S_Y = 0.25$ as we mentioned above and at the six locations ($x' = 0.0, 0.2, 0.4, 0.6, 0.8,$ and 0.9). The spectrum S_{hh}/S_{QQ} in Fig. 3a is more or less horizontal (i.e., white noise) at low frequencies and decrease gradually as f increases, indicating that an aquifer acts as

Analyses of uncertainties and scaling of groundwater level fluctuations

X. Liang and Y.-K. Zhang

Title Page

Abstract

Introduction

Conclusions

References

Tables

Figures

◀

▶

◀

▶

Back

Close

Full Screen / Esc

Printer-friendly Version

Interactive Discussion

Analyses of uncertainties and scaling of groundwater level fluctuations

X. Liang and Y.-K. Zhang

Title Page

Abstract

Introduction

Conclusions

References

Tables

Figures

◀

▶

◀

▶

Back

Close

Full Screen / Esc

Printer-friendly Version

Interactive Discussion

a low-bass filter that filter signals at high frequencies and keep signals at low frequencies. The aquifer has significantly dampened the fluctuations of the groundwater level. The spectrum varies with the location x' : the smaller the value of x' or the closer to the left flux boundary ($x' = 0$), the larger the spectrum (Fig. 3a–c). All spectra in Fig. 3a are not a straight line in the log-log plot, meaning that the temporal scaling of $h(x, t)$ does not exist in the range of $f = 10^{-3} \sim 10^0$ when $t_c = 40$ days. As t_c increases to 400 and 4000 days, however, the spectrum at $x' = 0$ become a straight line (the top curve in Fig. 3b and c) or has a power-law relation with f , i.e., $S_{hh}/S_{QQ} \propto 1/f$, since its slope is approximately one. The fluctuations of $h(0, t)$ is a pink noise due to the white noise fluctuations flux boundary when the characteristic timescale (t_c) is large which means that the aquifer is relatively less permeable and/or has a much larger horizontal length than its thickness.

Secondly, the spectrum S_{hh}/S_{HH} due to the sole effect of the random head boundary was evaluated by setting $S_{HH} \neq 0$, $S_{WW} = 0$, and $S_{QQ} = 0$ in Eq. (11) for the same three values of t_c and six locations and presented in Fig. 3d–f as a function of f . It is shown that similar to Fig. 3a–c, the spectrum decreases as f increases but different from Fig. 3a–c, the spectrum is larger at $x' = 0.9$ near the right boundary (the top curves in Fig. 3d–f) than that $x' = 0.0$ (the bottom curves). Furthermore, none of the spectra are a straight line in the log-log plot, indicating that the temporal scaling of groundwater level fluctuations does not exist in the case of the white noise head boundary.

Thirdly, the spectrum S_{hh}/S_{WW} due the effect of the white noise recharge only was evaluated by setting $S_{WW} \neq 0$, $S_{QQ} = 0$, and $S_{HH} = 0$ in Eq. (11) for the same values of t_c and x' and presented in Fig. 3g–i as a function of f . It is shown that when $t_c = 40$ day the spectrum in Fig. 3g is horizontal at low frequencies and become a straight line at high frequencies: the closer to the right head boundary, the later it approaches a straight line (Fig. 3h). As t_c increases to 400 and 4000 days, the slope of the spectrum at all locations except at $x' = 0.9$ approaches to a straight line with a slope of 2 (Fig. 3h and i), indicating a temporal scaling of $h(x, t)$. The fluctuations of groundwater level is

a Brownian motion, i.e., $S \propto 1/f^2$, when $t_c \geq 4000$ day or in a relatively less permeable and/or has a much larger horizontal length than its thickness.

Finally, the head spectrum due to the combined effect of all three random sources (the white noise recharge, and flux and head boundaries) was evaluated, i.e., $S_{WW} \neq 0$, $S_{QQ} \neq 0$, and $S_{HH} \neq 0$ in Eq. (11). The spectrum of S_{hh}/S_{WW} as a function of f was presented in Fig. 4 for the same values of t_c and x' where $S_{QQ}/S_{WW} = 1000$ and $S_{HH}/S_{WW} = 10\,000$ which are same with the values using in previous section. It is noticed that the general patterns of S_{hh}/S_{WW} in the combined case (Fig. 4) is similar to the case under the random source/sink only (Fig. 3g–i) except at $x' = 0.0$ and 0.9 (the dashed and dotted curve in Fig. 4a, respectively) due to the strong effects of the boundary conditions at these two location. At $t_c = 4000$ day, the spectra at all locations except $x' = 0.0$ (Fig. 4c) are similar to those in Fig. 3i, indicating the dominating effect of the random areal source/sink. The spectrum at $x' = 0$ in this case is also a straight line (the dashed curve in Fig. 4c) but with a different slope due to the effect of the random flux boundary which is similar to the top straight line in Fig. 3c. Above results provide a theoretical explanation as why temporal scaling exists in the observed groundwater level fluctuations (Zhang and Schilling, 2004; Bloomfield and Little, 2010; Zhu et al., 2012). We thus conclude that temporal scaling of $h(x, t)$ may indeed exist in real aquifers due to the strong effect of the areal source/sink.

4 Conclusions

In this study the effects of random source/sink, and initial and boundary conditions on the uncertainty and temporal scaling of the groundwater level, $h(x, t)$ were investigated. The analytical solutions for the variance, covariance and spectrum of $h(x, t)$ in an unconfined aquifer described by a linearized Boussinesq equation with white noise source/sink, and initial and boundary conditions were derived. The standard deviations of $h(x, t)$ for various cases were evaluated. Based on the results, the following conclusions can be drawn.

HESSD

12, 1–23, 2015

Analyses of uncertainties and scaling of groundwater level fluctuations

X. Liang and Y.-K. Zhang

Title Page

Abstract

Introduction

Conclusions

References

Tables

Figures

◀

▶

◀

▶

Back

Close

Full Screen / Esc

Printer-friendly Version

Interactive Discussion



Analyses of uncertainties and scaling of groundwater level fluctuations

X. Liang and Y.-K. Zhang

[Title Page](#)

[Abstract](#)

[Introduction](#)

[Conclusions](#)

[References](#)

[Tables](#)

[Figures](#)

[⏪](#)

[⏩](#)

[◀](#)

[▶](#)

[Back](#)

[Close](#)

[Full Screen / Esc](#)

[Printer-friendly Version](#)

[Interactive Discussion](#)

1. The error in $h(x, t)$ due to a random initial condition is significant at early time, especially near a flux boundary (Fig. 1b). The duration during which the effect is significant may last a few hundred days in most aquifers;
2. The error in $h(x, t)$ due to a random areal source/sink is significant in most part of an aquifer (Fig. 1d). The closer to a flux boundary, the larger the error;
3. The errors in $h(x, t)$ due to random flux and head boundaries are significant near the boundaries (Fig. 1f and h): the closer to the boundaries, the larger the errors. The random flux boundary may affect the head over a larger region near the boundary than the random head boundary;
4. In the typical aquifer studied the error in $h(x, t)$ in early time is mainly caused by an uncertain initial condition and the error reduces as time goes to reach a constant error in later time (Fig. 2b). The constant error in $h(x, t)$ is mainly due to the combined effects of uncertain source/sink and boundaries;
5. The aquifer system behaves as a low-pass filter which filter the short-term (low frequencies) fluctuations and keep the long-term (low frequencies) fluctuations;
6. Temporal scaling of groundwater level fluctuations may indeed exist in most part of a low permeable aquifer whose horizontal length is much larger than its thickness caused by the temporal fluctuations of areal source/sink.

Finally, it is pointed out that the analyses carried out in this study is under the assumptions that the processes, $W(t)$, $Q(t)$, and $H(t)$ are uncorrelated white noises. In reality, they may be correlated and spatially varied. We plan to relax those constrains and study more realistic cases in the near future.

Acknowledgements. This study was partially supported with the research grants from the National Nature Science Foundation of China (NSFC-41272260; NSFC-41330314; NSFC-41302180), the Natural Science Foundation of Jiangsu Province (SBK201341336) and from the National Key project “Water Pollution Control in the Huai River Basin” of China (2012ZX07204-001, 2012ZX07204-003).

References

- Bear, J.: Dynamics of Fluids in Porous Media, Environmental Science Series (New York, 1972), American Elsevier Pub. Co., New York, XVII, 764 pp., 1972.
- Beven, K. and Binley, A.: The future of distributed models – model calibration and uncertainty prediction, *Hydrol. Process.*, 6, 279–298, 1992.
- Bloomfield, J. P. and Little, M. A.: Robust evidence for random fractal scaling of groundwater levels in unconfined aquifers, *J. Hydrol.*, 393, 362–369, doi:10.1016/j.jhydrol.2010.08.031, 2010.
- Dagan, G.: Flow and Transport in Porous Formations, Springer-Verlag, Berlin, New York, XVII, 465 pp., 1989.
- Gelhar, L. W.: Stochastic Subsurface Hydrology, Prentice-Hall, Englewood Cliffs, NJ, X, 390 pp., 1993.
- Hantush, M. M. and Marino, M. A.: One-dimensional stochastic-analysis in leaky aquifers subject to random leakage, *Water Resour. Res.*, 30, 549–558, doi:10.1029/93wr02887, 1994.
- Liang, X. Y. and Zhang, Y. K.: A new analytical method for groundwater recharge and discharge estimation, *J. Hydrol.*, 450, 17–24, doi:10.1016/j.jhydrol.2012.05.036, 2012.
- Liang, X. Y. and Zhang, Y. K.: Temporal and spatial variation and scaling of groundwater levels in a bounded unconfined aquifer, *J. Hydrol.*, 479, 139–145, doi:10.1016/j.jhydrol.2012.11.044, 2013.
- Neuman, S. P.: Maximum likelihood Bayesian averaging of uncertain model predictions, *Stoch. Env. Res. Risk A*, 17, 291–305, doi:10.1007/s00477-003-0151-7, 2003.
- Neuman, S. P., Xue, L., Ye, M., and Lu, D.: Bayesian analysis of data-worth considering model and parameter uncertainties, *Adv. Water Resour.*, 36, 75–85, doi:10.1016/j.advwatres.2011.02.007, 2012.
- Priestley, M. B.: Spectral Analysis and Time Series, Academic Press, San Diego, 1981.
- Refsgaard, J. C., van der Sluijs, J. P., Hojberg, A. L., and Vanrolleghem, P. A.: Uncertainty in the environmental modelling process – a framework and guidance, *Environ. Modell. Softw.*, 22, 1543–1556, doi:10.1016/j.envsoft.2007.02.004, 2007.
- Rojas, R., Feyen, L., and Dassargues, A.: Conceptual model uncertainty in groundwater modeling: combining generalized likelihood uncertainty estimation and Bayesian model averaging, *Water Resour. Res.*, 44, W12418, doi:10.1029/2008wr006908, 2008.

HESSD

12, 1–23, 2015

Analyses of uncertainties and scaling of groundwater level fluctuations

X. Liang and Y.-K. Zhang

[Title Page](#)

[Abstract](#)

[Introduction](#)

[Conclusions](#)

[References](#)

[Tables](#)

[Figures](#)

[⏪](#)

[⏩](#)

[◀](#)

[▶](#)

[Back](#)

[Close](#)

[Full Screen / Esc](#)

[Printer-friendly Version](#)

[Interactive Discussion](#)



Analyses of uncertainties and scaling of groundwater level fluctuations

X. Liang and Y.-K. Zhang

[Title Page](#)

[Abstract](#)

[Introduction](#)

[Conclusions](#)

[References](#)

[Tables](#)

[Figures](#)

[⏪](#)

[⏩](#)

[◀](#)

[▶](#)

[Back](#)

[Close](#)

[Full Screen / Esc](#)

[Printer-friendly Version](#)

[Interactive Discussion](#)



- Rojas, R., Feyen, L., Batelaan, O., and Dassargues, A.: On the value of conditioning data to reduce conceptual model uncertainty in groundwater modeling, *Water Resour. Res.*, 46, W08520, doi:10.1029/2009wr008822, 2010.
- Schilling, K. E. and Zhang, Y. K.: Temporal scaling of groundwater level fluctuations near a stream, *Ground Water*, 50, 59–67, doi:10.1111/j.1745-6584.2011.00804.x, 2012.
- Vrugt, J. A., Gupta, H. V., Bouten, W., and Sorooshian, S.: A shuffled complex evolution metropolis algorithm for optimization and uncertainty assessment of hydrologic model parameters, *Water Resour. Res.*, 39, 1201, doi:10.1029/2002wr001642, 2003.
- Ye, M., Meyer, P. D., and Neuman, S. P.: On model selection criteria in multimodel analysis, *Water Resour. Res.*, 44, W03428, doi:10.1029/2008wr006803, 2008.
- Zeng, X. K., Wang, D., Wu, J. C., and Chen, X.: Reliability analysis of the groundwater conceptual model, *Hum. Ecol. Risk Assess.*, 19, 515–525, doi:10.1080/10807039.2012.713822, 2013.
- Zhang, D.: *Stochastic Methods for Flow in Porous Media: Coping with Uncertainties*, Academic, San Diego, CA, London, XIV, 350 pp., 2002.
- Zhang, Y. K. and Li, Z. W.: Temporal scaling of hydraulic head fluctuations: nonstationary spectral analyses and numerical simulations, *Water Resour. Res.*, 41, W07031, doi:10.1029/2004wr003797, 2005.
- Zhang, Y. K. and Li, Z. W.: Effect of temporally correlated recharge on fluctuations of groundwater levels, *Water Resour. Res.*, 42, W10412, doi:10.1029/2005wr004828, 2006.
- Zhang, Y. K. and Schilling, K.: Temporal scaling of hydraulic head and river base flow and its implication for groundwater recharge, *Water Resour. Res.*, 40, W03504, doi:10.1029/2003wr002094, 2004.
- Zhang, Y. K. and Yang, X. Y.: Effects of variations of river stage and hydraulic conductivity on temporal scaling of groundwater levels: numerical simulations, *Stoch. Env. Res. Risk A*, 24, 1043–1052, doi:10.1007/s00477-010-0437-5, 2010.
- Zhu, J. T., Young, M. H., and Osterberg, J.: Impacts of riparian zone plant water use on temporal scaling of groundwater systems, *Hydrol. Process.*, 26, 1352–1360, doi:10.1002/Hyp.8241, 2012.

Analyses of uncertainties and scaling of groundwater level fluctuations

X. Liang and Y.-K. Zhang

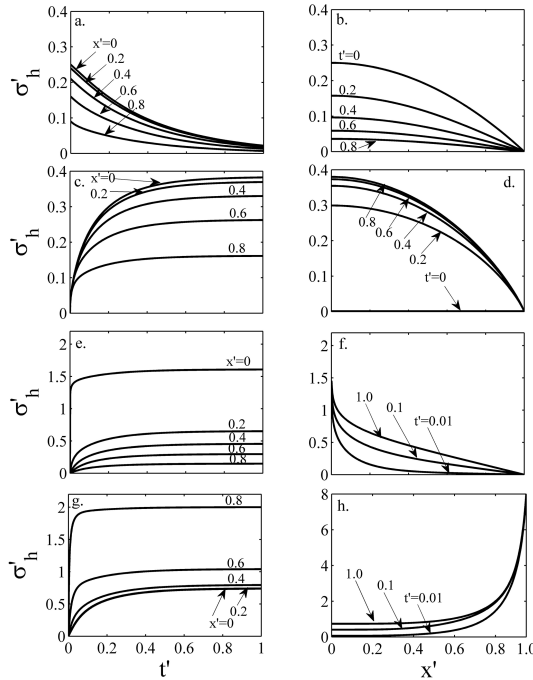


Figure 1. The standard deviation (σ'_h) of $h(x,t)$ vs. the dimensionless time (t') at the dimensionless locations $x' = 0.0, 0.2, 0.4, 0.6,$ and 0.8 (the four graphs in the left column) and the standard deviation (σ'_h) of $h(x,t)$ vs. the dimensionless location (x') for the dimensionless time $t' = 0.01, 0.1,$ and 1.0 (the four graphs in the right column): **(a)** and **(b)** are based on Eq. (12) where $\sigma_{W_0}^2 = \sigma_Q^2 = \sigma_H^2 = 0$; **(c)** and **(d)** are based on Eq. (13) where $\sigma_{W_0}^2 = \sigma_Q^2 = \sigma_H^2 = 0$; **(e)** and **(f)** are based on Eq. (13) where $\sigma_{W_0}^2 = \sigma_W^2 = \sigma_H^2 = 0$; **(g)** and **(h)** are based on Eq. (15) where $\sigma_{W_0}^2 = \sigma_W^2 = \sigma_Q^2 = 0$.

[Title Page](#)
[Abstract](#) [Introduction](#)
[Conclusions](#) [References](#)
[Tables](#) [Figures](#)
[◀](#) [▶](#)
[◀](#) [▶](#)
[Back](#) [Close](#)
[Full Screen / Esc](#)
[Printer-friendly Version](#)
[Interactive Discussion](#)



Analyses of uncertainties and scaling of groundwater level fluctuations

X. Liang and Y.-K. Zhang

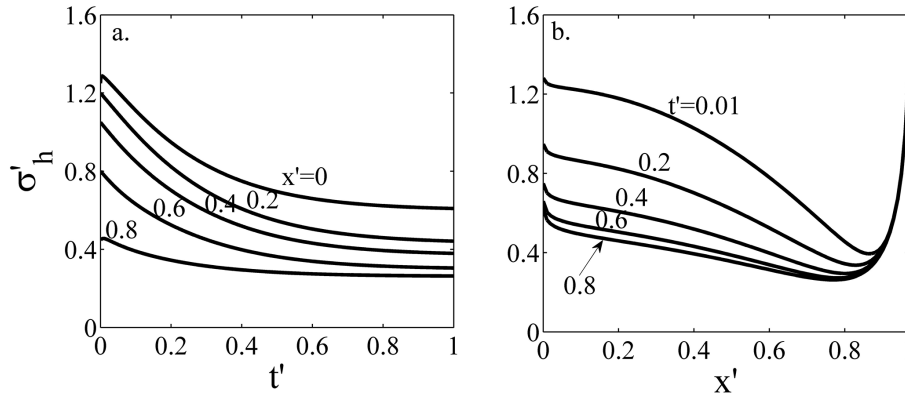


Figure 2. (a) The standard deviation (σ'_h) of $h(x, t)$ vs. the dimensionless time (t') at the dimensionless locations $x' = 0.0, 0.2, 0.4, 0.6,$ and 0.8 and (b) the standard deviation (σ'_h) of $h(x, t)$ vs. the dimensionless location (x') for the dimensionless time $t' = 0.01, 0.1,$ and $1.0,$ evaluated based on Eq. (16) where $\sigma_{W_0}^2 \neq \sigma_W^2 \neq \sigma_Q^2 \neq \sigma_H^2 \neq 0$.

Title Page	
Abstract	Introduction
Conclusions	References
Tables	Figures
◀	▶
◀	▶
Back	Close
Full Screen / Esc	
Printer-friendly Version	
Interactive Discussion	

Analyses of uncertainties and scaling of groundwater level fluctuations

X. Liang and Y.-K. Zhang

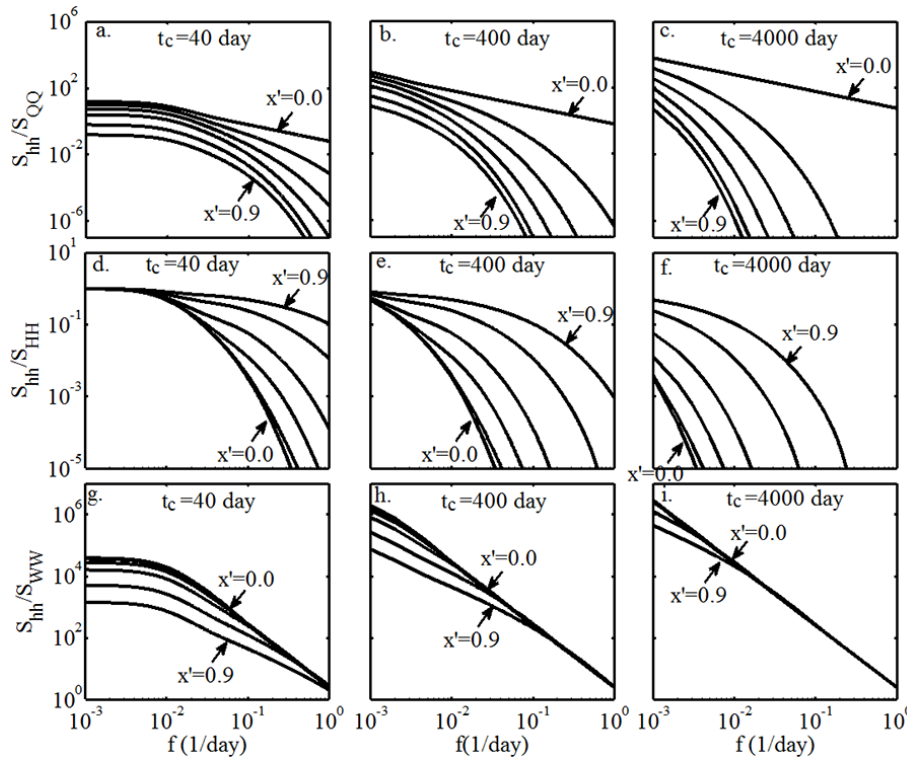


Figure 3. The dimensionless power spectrum vs. frequency (f) at the dimensionless locations $x' = 0.0, 0.2, 0.4, 0.6, 0.8,$ and 0.9 . The left column is for $t_c = 40$ day, the middle column is for $t_c = 400$ day, and the right column is for $t_c = 4000$ day. The first row is the dimensionless spectrum S_{hh}/S_{QQ} when $S_{WW} = 0$, $S_{HH} = 0$, and $S_{QQ} \neq 0$ in Eq. (11), the second row is S_{hh}/S_{HH} when $S_{WW} = 0$, $S_{QQ} = 0$, and $S_{HH} \neq 0$, and the bottom row is S_{hh}/S_{WW} when $S_{QQ} = 0$, $S_{HH} = 0$, and $S_{WW} \neq 0$.

Title Page

Abstract	Introduction
Conclusions	References
Tables	Figures

⏪
⏩

◀
▶

Back	Close
------	-------

Full Screen / Esc

Printer-friendly Version

Interactive Discussion



Analyses of uncertainties and scaling of groundwater level fluctuations

X. Liang and Y.-K. Zhang

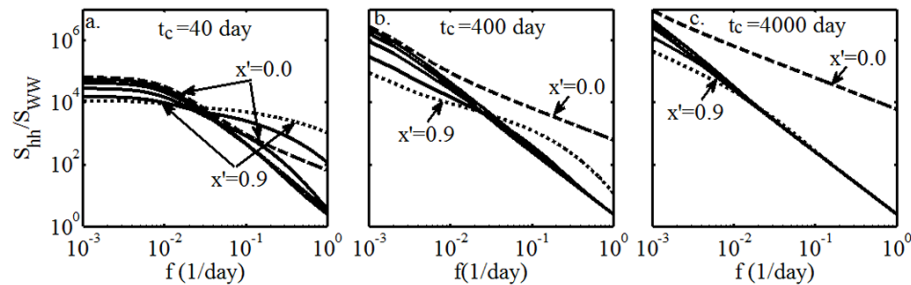


Figure 4. The dimensionless power spectrum vs. frequency (f) at the dimensionless locations $x' = 0.0, 0.2, 0.4, 0.6, 0.8,$ and 0.9 when $S_{QQ} \neq 0$, $S_{HH} \neq 0$, and $S_{WW} \neq 0$ for **(a)** $t_c = 40$ day, **(b)** $t_c = 400$ day, and **(c)** $t_c = 4000$ day.

Title Page

Abstract

Introduction

Conclusions

References

Tables

Figures

◀

▶

◀

▶

Back

Close

Full Screen / Esc

Printer-friendly Version

Interactive Discussion